Lattice Boltzmann model for the Elder problem

D.T. Thorne[a] and M.C. Sukop[a]

[a]Department of Earth Sciences, Florida International University,
PC 344, University Park, 11200 SW 8th Street, Miami, Fl 33199

Lattice Boltzmann models are rapidly proving their ability to simulate many fluid dynamics problems that previously required far more complex approaches. We use a multicomponent model to address the classic solute-induced buoyancy Elder problem (transient solute/density-induced convection in porous media), which has been widely adopted as a "benchmark" problem among density-dependent flow modelers. This work represents first steps in the development of lattice Boltzmann models for application to groundwater problems (e.g., salt-water intrusion) in coastal regions.

1. INTRODUCTION

Groundwater flows in coastal regions present simulation challenges arising from interactions between low-density fresh water and high density seawater [11,9,14]. Groundwater models for use in these areas must be able to simulate density driven flow, solute advection, diffusion, and dispersion (e.g., where seawater and fresh water mix) in porous media. Lattice Boltzmann Methods (LBMs) offer a new computational tool that has not previously been applied to seawater intrusion problems to our knowledge. In our opinion, LBMs offer a radically simpler approach for such problems. The steps outlined in §2 are much simpler to implement than conventional (e.g., finite element) methods. A novice programmer (or even an industrious non-programmer, perhaps) can implement a usable LBM code.

In the results reported here, we validate LBMs on the classic Elder problem of density driven flows in porous media [7,8], in the spirit of SUTRA, SEAWAT, and others [10,12]. Elder introduced the problem in 1967 [7,8] to study convection in porous media due to non-uniform heating. Since then it has been widely adapted for use by the hydrogeology community [10,11,9,14] The Elder problem is a 2-D problem, and a 2-D LBM suffices for its simulation.

An introduction to LBMs is provided in §2. A technique for using a multicomponent LBM to simulate solute transport is described in §3. Simulation of porous media is discussed in §4. Results for the Elder problem and comparisons with previous results are given in §5, followed by closing remarks in §6.

2. LBM PRIMER

Detailed descriptions of LBMs can be found in [2,1]. We present a brief outline here and cite more specialized literature where appropriate.

LBMs are implemented on a discrete set of regularly spaced spatial locations called a lattice. Each node in the lattice has an associated particle distribution function that represents the probability of particles being at that lattice node with a given velocity at the current time step. The distribution function describes probabilities over a discrete set of velocities, including a zero velocity (allowing "rest" particles). The macroscopic density and velocity of the simulated fluid are computed from the particle distribution function (see below).

Commonly, 2-D LBMs are implemented on either hexagonal or rectangular lattices. We work on a rectangular lattice with nine velocities (including the zero velocity for "rest" particles), as illustrated in Fig. 1. This is usually referred to as the D2Q9 model, signifying

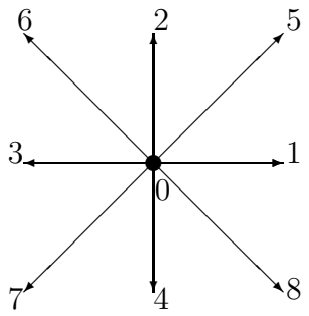

Figure 1. D2Q9

two dimensions and nine discrete velocities:

$$\begin{cases} \mathbf{e}_6 = (-1,1), & \mathbf{e}_2 = (0,1), & \mathbf{e}_5 = (1,1), \\ \mathbf{e}_3 = (-1,0), & \mathbf{e}_0 = (0,0), & \mathbf{e}_1 = (1,0), \\ \mathbf{e}_7 = (-1,-1), & \mathbf{e}_4 = (0,-1), & \mathbf{e}_8 = (1,-1). \end{cases} \tag{1}$$

We denote the distribution in the a^{th} direction by f_a for $0 \leq a \leq 8$, where $a = 0$ is the rest direction. Density ρ and velocity $\mathbf{u}$ of the fluid are recovered from the distribution function as

$$\rho = \sum_{a=0}^{8} f_a \tag{2}$$

and

$$\mathbf{u} = \frac{1}{\rho} \sum_{a=0}^{8} f_a \mathbf{e}_a. \tag{3}$$

The particle distribution is a function of position and time, so $f_a = f_a(\mathbf{x}, t)$, where $\mathbf{x}$ is the coordinate of a lattice node and t is a time step. Each time step t consists of a

streaming step and a *collision* step. In the streaming step, the distributions are copied to adjacent lattice sites in their respective directions. Viewing streaming as an intermediate step, we can denote its result by f^*,

$$f_a^*(\mathbf{x}+\mathbf{e}_a,t) = f_a(\mathbf{x},t), 1 \le a \le 8. \tag{4}$$

Collisions are then simulated based on a special *equilibrium distribution function* (see [2,1]) to compute the distribution function at the new time step:

$$f_a(\mathbf{x},t+\Delta t) = f_a^*(\mathbf{x},t) + \frac{1}{\tau}\left(f_a^{eq}(\mathbf{x},t) - f_a^*(\mathbf{x},t)\right), 0 \le a \le 8, \tag{5}$$

where f^{eq} is the equilibrium distribution function

$$f_a^{eq} = E_a\rho\left[1 + 3\mathbf{c}_a\cdot\mathbf{u} + \frac{9}{2}(\mathbf{c}_a\cdot\mathbf{u})^2 - \frac{3}{2}\mathbf{u}\cdot\mathbf{u}\right] \tag{6}$$

with

$$E_a = \begin{cases} \frac{4}{9} & \text{for } a = 0, \\ \frac{1}{9} & \text{for } a \in \{1,2,3,4\}, \\ \frac{1}{36} & \text{for } a \in \{5,6,7,8\}, \end{cases} \tag{7}$$

and τ is known as the relaxation time in this BGK formulation [2]. It relates to the kinematic viscosity ν of the simulated fluid as

$$\nu = \frac{1}{3}\left(\tau - \frac{1}{2}\right). \tag{8}$$

With this equilibrium distribution function, it has been shown that, under certain assumptions (e.g., low Mach number), this process is a second order approximation to the solution of the Navier-Stokes equation [4,2,1].

Note that the time stepping begins with f set equal to f^{eq}, $f \leftarrow f^{eq}$.

Body forces such as gravity are implemented as an addition to the velocity vector used to compute f^{eq} [6]. Let $\mathbf{u}^*$ denote the intermediate velocity computed as

$$\mathbf{u}^* = \frac{1}{\rho}\sum_{a=0}^{8} f_a\mathbf{e}_a \tag{9}$$

with f from the last time step. Then f^{eq} is computed using

$$\mathbf{u} = \mathbf{u}^* + \tau g. \tag{10}$$

The only boundary condition we need for the fluid is a no-slip condition at walls. This is implemented with the common "bounce-back" technique [2,1].

3. SOLUTE TRANSPORT

In [3], Yoshino and Inamuro present a method for simulating solute transport using a second component, hereafter referred to as the solute component or σ-component. We denote the distribution function of the solute component by f_σ. The solute distribution function f_σ is updated in the streaming step and collision step in the same way as the fluid

distribution function f, except that f_σ has a separate relaxation time τ_σ and a different equilibrium distribution function:

$$f^{eq}_{\sigma,\,a} = E_a \rho_\sigma \left(1 + 3\mathbf{e}_a \cdot \mathbf{u}\right), \tag{11}$$

where E_a is the same as in §2.

The density ρ_σ of the solute component is computed the same way as the density of the fluid:

$$\rho_\sigma = \sum_{a=0}^{8} f_{\sigma,\,a}. \tag{12}$$

The mass diffusivity D_σ of the solute component is related to τ_σ by

$$D_\sigma = \frac{1}{3}\left(\tau_\sigma - \frac{1}{2}\right), \tag{13}$$

analogously to kinematic viscosity ν for the fluid component.

The solute component contributes to the flow through the gravity term in

$$\mathbf{u} = \mathbf{u}^* + \tau g \frac{\rho + \rho_\sigma}{\rho}, \tag{14}$$

which is an adjustment to equation (10).

For the implementation of concentration boundary conditions needed by the Elder problem in §5, see [3].

4. POROUS MEDIA

A porous medium permits the flow of fluid in proportion to its permeability. Dardis and McCloskey [4,5] introduce a volumetric solids fraction parameter n_s, $0 \le n_s \le 1$, along with a new step in the LB procedure to damp the evolution of momentum in proportion to n_s, thereby simulating a porous medium with porosity $1 - n_s$ in which permeability is inversely proportional to the solids fraction (see equation (17)). In simplistic terms, this method can be viewed as a probabilistic microscopic bounce-back in response to the fractional solid density.

The new porous media step takes place after the traditional collision step. Considering the traditional collision step as a second intermediate step after streaming, let f^{**} denote the result of the collision step

$$f^{**}_a(\mathbf{x}, t + \Delta t) = f^*_a(\mathbf{x}, t) + \frac{1}{\tau}\left(f^{eq}_a(\mathbf{x}, t) - f^*_a(\mathbf{x}, t)\right), 0 \le a \le 8. \tag{15}$$

Then the porous media step has the form

$$f_a(\mathbf{x}, t+\Delta t) = f^{**}_a(\mathbf{x}, t+\Delta t) + n_s\left[f^{**}_{a'}(\mathbf{x} + \mathbf{e}_a\Delta t, t + \Delta t) - f^{**}_a(\mathbf{x}, t + \Delta t)\right], 1 \le a \le 8, \tag{16}$$

where a' is the index of the direction opposite $\mathbf{e}_a$. Note that n_s can be a function of $\mathbf{x}$, $n_s = n_s(\mathbf{x})$, which allows great flexibility in porous medium simulations — fractured porous media can be readily simulated, for example. However, n_s is simply a constant for the homogeneous medium we study here.

If $n_s = 0$, the porous media step clearly has no effect, and the process reduces to the usual free-fluid LBM. If $n_s = 1$, then

$$\begin{aligned} f_a(\mathbf{x}, t+\Delta t) &= f_a^{**}(\mathbf{x}, t+\Delta t) + f_{a'}^{**}(\mathbf{x}+\mathbf{e}_a\Delta t, t+\Delta t) - f_a^{**}(\mathbf{x}, t+\Delta t) \\ &= f_{a'}^{**}(\mathbf{x}+\mathbf{e}_a\Delta t, t+\Delta t) \\ &= \frac{1}{\tau}\left[f_{a'}^{*}(\mathbf{x}+\mathbf{e}_a\Delta t, t) - f_{a'}^{eq}(\mathbf{x}+\mathbf{e}_a\Delta t, t)\right] = 0, \end{aligned}$$

since $f \leftarrow f^{eq}$ in the beginning, thus eliminating flow altogether, as expected.

Dardis and McCloskey [4] show that the permeability k of a medium with solid density n_s can be computed as

$$k = \frac{\nu}{2n_s}. \tag{17}$$

We apply the porous media step is applied only to the fluid component, not the solute component.

5. ELDER PROBLEM

Elder introduced the problem in 1967 [7,8] to study convection in porous media due to non-uniform heating. Since then, the solutal analog of the Elder problem has been widely adapted for use by the hydrogeology community [10,11,9,14].

The configuration of the Elder problem is shown in Fig. 2. A horizontal slab of homogeneous porous material of thickness H and horizontal extent E forms the domain. The walls of the slab are impermeable. The bottom wall is held at concentration $C_0 = 0$ and a region of width L in the center of the top wall is held at $C_0 + \Delta C$ ($= 0 + 1$, as

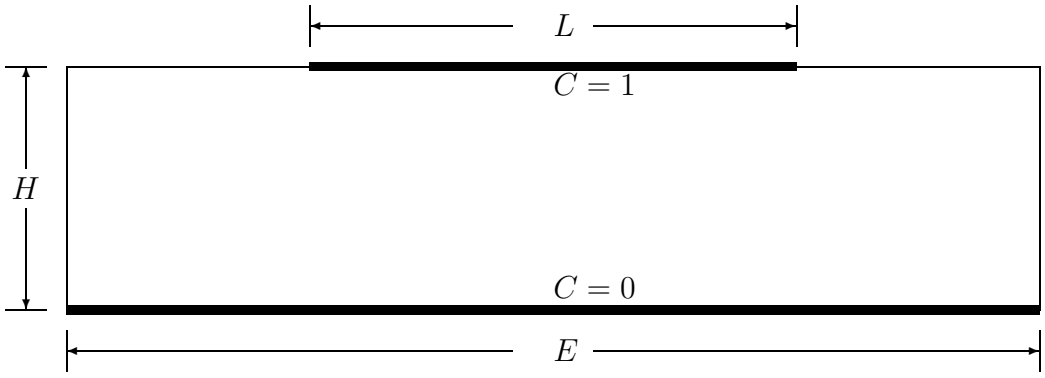

Figure 2. Configuration of the Elder problem. Homogeneous porous material, thickness H, horizontal extent E. Impermeable walls. Bottom concentration $C_0 = 0$, concentration $C = 1$ on region of length L at top.

a non-dimensional concentration). The non-dimensional concentration of the solute is related to the dimensional concentration through the equation of state [12,10]

$$\rho = 1000 \text{ kg m}^{-3} + (200 \text{ kg m}^{-3})C, \tag{18}$$

which relates the concentration and density of the fluid.

Elder [8] used the traditional Rayleigh non-dimensional number to quantify the temperature-induced density-driven onset of convection. The solute induced buoyancy problem can be characterized by the solutal Rayleigh number for porous media:

$$Ra = \frac{k\gamma g H \Delta C}{\nu \phi D}, \tag{19}$$

where k is the permeability, γ is the solutal expansion coefficient, g is the acceleration due to gravity, H is the horizontal extent of the domain, ΔC is the maximum difference in non-dimensional concentration of solute, ν is the kinematic viscosity, ϕ is the porosity, and D is the molecular diffusivity.

All of our dimensions are measured in terms of the lattice. Length is denoted by lu for lattice units. Mass is denoted by mu for mass units. Time is denoted by ts for time steps.

The solutal expansion coefficient γ is the derivative of the equation of state (18) at constant pressure and scaled by the reference density

$$\gamma = \frac{1}{\rho_0}\left(\frac{\partial \rho}{\partial C}\right)_P = \frac{200}{1000} = 0.2. \tag{20}$$

The intrinsic permeability, in units of lu^2, is computed as in [4]: $k = \frac{\nu}{2n_s}$.

The entire parameter set is shown in Table 1 with values chosen to match Elder's

Table 1
Elder problem parameters for LBM and conventional models.

	LB Units	Common Units
k	1.852×10^{-6} lu^2	4.845×10^{-13} m^2
γ	.2	.2
g	2.512×10^{-3} lu ts^{-2}	9.81 m s^{-2}
H	20 lu	150 m
ΔC	1	1
ν	3.333×10^{-6} lu^2 ts^{-1}	1.0×10^{-6} m^2 s^{-1}
ϕ	.1	.1
D	1.396×10^{-4} lu^2 ts^{-1}	3.565×10^{-6} m^2 s^{-1}

classic $Ra = 400$ case [8]. The table gives our choice of values in the Lattice Boltzmann framework along side the common values used by others [10,9,11,12]. Clearly, no set of parameters is unique, and identical Ra can be achieved for different values. As long as Ra is equal, however, the physical process simulated should be the same. Following is the computation of the Rayleigh number using the LB-based parameters:

$$Ra = \frac{k\gamma g H \Delta C}{\nu \phi D} = \frac{(0.00000185 \text{ lu}^2)(.2)(.002512 \text{ lu ts}^{-2})(20 \text{ lu})(1)}{(0.00000333 \text{ lu}^2 \text{ ts}^{-1})(.1)(0.0001396 \text{ lu}^2 \text{ ts}^{-1})} \approx 400. \tag{21}$$

And here is the computation of the Rayleigh number using the common parameter set:

$$Ra = \frac{k\gamma g H \Delta C}{\nu \phi D} = \frac{(4.845 \times 10^{-13}\ \mathrm{m}^2)(.2)(9.81\ \mathrm{m\ s}^{-2})(150\ \mathrm{m})(1)}{(1.0 \times 10^{-6}\ \mathrm{m}^2\ \mathrm{s}^{-1})(.1)(3.565 \times 10^{-6}\ \mathrm{m}^2\ \mathrm{s}^{-1})} \approx 400. \tag{22}$$

In Fig. 3, our results are shown with Elder's results. Elder presents contours at $C = .2$

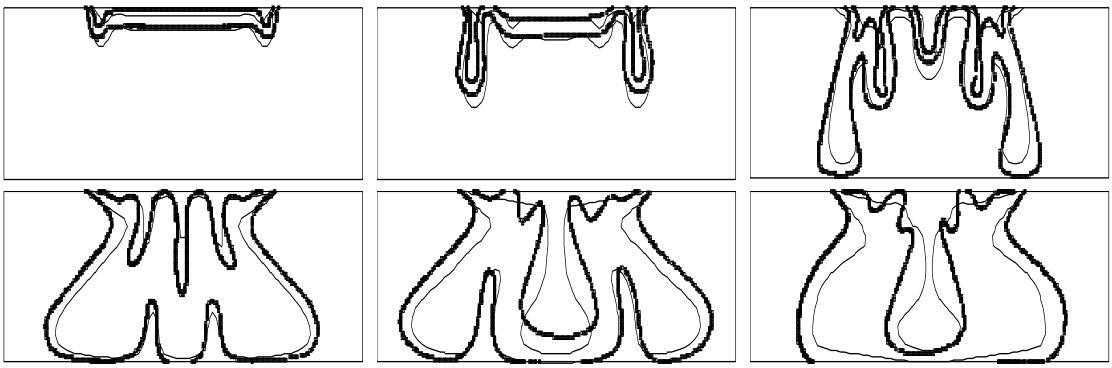

Figure 3. Plots with Elder style aspect ratio at years 1, 2, 4, 10, 15 and 20. Concentrations are shown at $C = .2$ and $C = .6$. The dark lines are Elder's results, and the thin lines are our results.

and $C = .6$ in a box with the horizontal scale reduced by a factor of two.

In Fig. 4, our results are shown with Frolkovič and Schepper's proposed "reference"

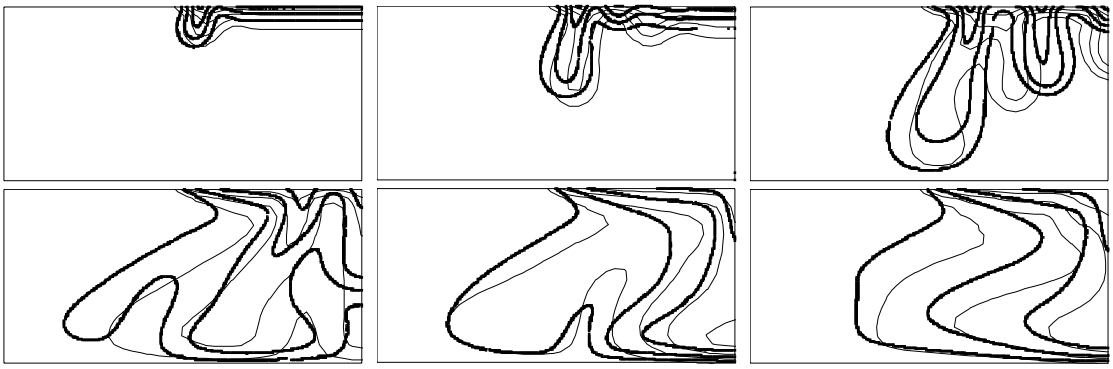

Figure 4. Plots of half the domain in the style of [9] at years 1, 2, 4, 10, 15 and 20. Concentrations are shown at $C = .2$, $C = .4$, $C = .6$, and $C = .8$. The dark lines are Frolkovič and Schepper's results, and the thin lines are our results.

solutions. Frolkovič and Schepper present contours at $C = .2$, $C = .4$, $C = .6$, and $C = .8$ on half of the domain with the same scale on the vertical and horizontal axes.

We estimated the number of time steps per year by matching with the results of Frolkovič and Schepper [9]. Our independent computations of dimensional elapsed time differed by approximately a factor of three.

Because of the numerical difficulties inherent in simulations involving non-linear, coupled solute transport and density-driven flow, inconsistent numerical results have often been reported in the literature [9,14,10]. Kolditz et al. [13] provided a list of 12 numerical variable density groundwater flow and transport simulators. At least one additional model, SEAWAT [12], has recently come into widespread use. Analytical solutions for the problems addressed by these models are rarely available, and validation of the various codes has generally relied on comparison with previous numerical results [13]. Three "benchmark problems", including the Henry problem, the Elder problem, and the HYDROCOIN problem, are generally considered. As in [9], we limit our consideration to the Elder problem in this paper. In what we believe to be the most numerically advanced and sophisticated Elder problem simulations using a standard continuum modeling framework, Frolkovič and Schepper [9] investigated the dependence of the results on grid refinement, numerical scheme, and numerical perturbations.

We wish to emphasize that, although the Elder problem has been so widely adopted as a "benchmark," there is controversy about its usefulness [14] because there is no reliable solution to date. There is no solution to the Elder problem that is known to be accurate. The results of the myriad published numerical experiments are highly variable, being extremely sensitive to the numerical method, the discretization (in both space and time), and the initial conditions. Furthermore, the difficulty in doing the experiment in the (actual, physical) laboratory makes those results also questionable. Woods et al. [14] point out that "the extent to which either the laboratory work or Elder's numerical solution can be trusted remains an open question." Not only is there no fully trustworthy solution to the Elder problem, but there may not even be a unique solution. Frolkovič and Schepper's [9] results suggest that there may be multiple non-unique solutions to the Elder problem. This is not unprecedented. A similar problem, Bènard convection, has been proven to have multiple non-unique solutions [9].

In light of this, our results make us very optimistic about the viability of Lattice Boltzmann methods for simulating this type of problem. We note that Woods et al. [14] suggest that replication of the Frolkovič and Schepper very high resolution results [9] could lead to a more definitive solution to the Elder problem. Though our results match neither Elder's nor Frolkovič and Schepper's, the overall behavior is the same. We expect that LBMs may have a significant impact on the solution of the type of density driven flow represented by the Elder problem. In addition to that, it is our hope that by suggesting the application of a new tool we are contributing to the process of resolving the uncertainties associated with the Elder problem. While the results that we present in this paper do not help to validate any particular proposed solution to the Elder problem (e.g., [9]) as the right one, we are anxious to do more experiments. We observe that an important advantage of LBMs is that they can support arbitrarily high resolution without catastrophic roundoff error. This is due to the fact that LBMs are not computed in terms of a mesh spacing in the way that conventional discretizations of the macroscopic equations are. The roundoff errors associated with the LBM steps (streaming and collision) outlined in §2 are unchanged by the size of the lattice.

6. CONCLUSIONS

Groundwater flows in coastal regions present simulation challenges arising from interactions between low-density fresh water and high density seawater [11,9,14]. A groundwater model must be able to simulate density driven flows (e.g., where seawater and fresh water mix) in porous media.

Lattice Boltzmann Methods (LBMs) offer a new computational tool that has not previously been applied to seawater intrusion problems to our knowledge. Our study shows that LBMs are a highly viable tool for modeling seawater intrusion problems. Our results compare favorably with Elder's classic results and with modern state-of-the-art results such as those found in [9]. Moreover, LBMs have certain numerical advantages over conventional (e.g., finite element) methods for solving the highly non-linear coupled equations that govern these solute transport/density-driven flow problems.

REFERENCES

1. D.A. Wolf-Gladrow, Lattice-Gas Cellular Automata and Lattice Boltzmann Models: An Introduction, Springer, Berlin, 2000, 308pp.
2. S. Succi, The Lattice Boltzmann Equation for Fluid Dynamics and Beyond, Clarendon Press, Oxford, 2001, 288pp.
3. M. Yoshino, T. Inamuro, Int. J. Numer. Meth. Fluids 43 (2003) 183.
4. O. Dardis, J. McCloskey, Phys. Rev. E 57 (4) (1998) 4834–4837 April 1998.
5. O. Dardis, J. McCloskey, Geophysical Research Letters, Vol. 25, No. 9, Pages 1471-1474, May 1, 1998.
6. N.S. Martys, H. Chen, Phys. Rev. E 53 (1996) 743.
7. J. W. Elder, J. Fluid Mech., Vol. 27, Part 1, Pages 29–48, 1967.
8. J. W. Elder, J. Fluid Mech., Vol. 27, Part 3, Pages 609–623, 1967.
9. P. Frolkovič, H. De Schepper, Adv. Water Res. 24 (2001) 63–72.
10. C. I. Voss, W. R. Souza, Water Resources Research, Vol. 23, No. 10, Pages 1851–1866, October 1987.
11. C. M. Oldenburg, K. Pruess, Water Resources Research, Vol. 31, No. 2, Pages 289–302, February 1995.
12. W. Guo, C. D. Langevin, User's Guide to SEAWAT: A Computer Program for Simulation of Three-Dimensional Variable-Density Ground-Water Flow, U.S. Geological Survey, Techniques of Water-Resources Investigations 6-A7, Tallahassee, Florida, 2002.
13. O. Kolditz, R. Ratke, H. G. Diersch, W. Zielke, Advances in Water Resources, Vol. 21, No. 1, Pages 27–46, 1998.
14. J. A. Woods, M. D. Teubner, C. T. Simmons, K. A. Narayan, Water Resources Research, Vol. 39, No. 6, 1158, 2003.